Carbothermal Upgrading of the Awaso Bauxite Ore using Waste Pure Water Sachets as Reductant*

J. R. Dankwah, A.Y. Fosu, N. Fosu and P. Koshy

Dankwah, J. R., Fosu, A.Y., Fosu, N. and Koshy, P. (2015), “Carbothermal Upgrading of the Awaso Bauxite Ore using Waste Pure Water Sachets as Reductant”, *Ghana Mining Journal*, Vol. 15, No. 1, pp. 64 - 72.

Abstract

Waste Pure Water Sachets (PWS) are currently among the fastest growing solid wastes generated in Ghana. Government’s attempt at banning its production and usage has been thwarted by the realisation that such a measure will increase the unemployment rate since the sachet water business employs a significant proportion of people. Meanwhile, the country currently exports its bauxite raw, without any value addition. Gradual depletion of high grade bauxite (with high alumina content) and the emergence of low grade bauxite with high iron oxide content calls for novel and inexpensive ways to upgrade these low ores. This project investigates a simple way of generating carbonaceous materials from PWS and their subsequent utilisation as reductants in the carbothermal upgrading of the Ghana Awaso bauxite. Samples of PWS were heat-treated in the temperature range 130-180 °C and the resulting molten material was cooled to render it brittle. The brittle mass was then pulverised and characterised by XRD and SEM. Composite pellets of bauxite sample and pulverised PWS were then formed, oven dried, placed in a fireclay crucible and heated in a gas-fired furnace. The magnetic fraction after reduction was separated by a Low Intensity Magnet and weighed. XRD analyses of the pulverised PWS showed peaks identical to those of high density polyethylene (HDPE). It was further observed that after about 30 min of firing, a large portion of the sample could be attracted by the magnet, indicating the suitability of the waste polymer as an important carbonaceous material for bauxite upgrading. The use of PWS as reductant prevented the formation of hercynite ($FeAl_2O_4$).

Keywords: Pure water sachets, Bauxite, Gas-fired furnace, Magnetic fraction, High density polyethylene

1 Introduction

Waste Pure Water Sachets (PWS) are currently among the fastest growing solid wastes generated in Ghana, with virtually no proven avenues for their effective recycling. Government’s attempt at banning its production and usage has been thwarted by the realisation that such a measure will increase the unemployment rate since the sachet water business employs a significant proportion of people. Meanwhile, the country currently exports its bauxite raw, without any value addition. Gradual depletion of high grade bauxite (with high alumina content) and the emergence of low grade bauxite with high iron oxide content calls for novel and inexpensive ways to upgrade these low grade ores.

Bauxite is normally classified in accordance with the amount of water of crystallisation and crystal structure into gibbsite ($Al(OH)_3$), boehmite (γ-$AlO(OH)$), or diaspore (α-$AlO(OH)$). In addition to these hydroxides of aluminium, bauxite may contain varying amounts of iron oxides (typically goethite (FeOOH) and hematite (Fe_2O_3)), kaolinite, and some amounts of anatase or rutile (TiO_2) and quartz (SiO_2) (Kesse, 1985). The oxides of iron constitute the major impurity in bauxite and for the Awaso ore it typically ranges from about 7 wt % to as high as 50 wt %, depending on the location and depth. It is therefore important to remove or minimise the content of iron oxides prior to processing by the Bayer technology, in order to decrease the amount of waste generated as red mud. It has been estimated that if goethite and hematite could be recovered from bauxite as magnetite, the amount of red mud generated could be decreased by at least 40 wt.%, based on the composition of a typical red mud shown in Table 1. (Samouhos *et al.*, 2013).

Table 1 Chemical Composition of a Typical Bauxite Residue as Revealed by XRF (Samouhos *et al.*, 2013)

Component	Composition (wt.%)
SiO_2	7.37 ± 0.03
TiO_2	6.05 ± 0.01
Al_2O_3	14.63 ± 0.05
Fe_2O_3	43.19 ± 0.05
CaO	12.03 ± 0.03
MgO	0.31 ± 0.05
K_2O	0.07 ± 0.03
V_2O_5	0.16 ± 0.01
ZrO_2	1.12 ± 0.01
Na_2O	2.14 ± 0.03
Cr_2O_3	0.28 ± 0.01
LOI	12.19 ± 0.2

**Manuscript received March 30, 2015*
Revised version accepted May 17, 2015

Besides, iron oxide has the following detrimental effects on the alumina extraction process (Lu *et al.*, 2012):

(i) Separation of iron oxide from the aluminate liquor as red mud is difficult and slow because it is usually present in a finely disseminated form.

(ii) The leaching of alumina by caustic soda is favoured at high temperatures but increasing the temperature results in a simultaneous dissolution of iron oxide, leading to unnecessary reagent consumption.

(iii) Iron oxide interferes with the recovery of other impurities like titanium oxide.

The upgrading of low grade bauxite ores has been examined before by some investigators (Lu *et al.*, 2007; Lu *et al.*, 2012; Ye *et al.*, 2013; Reddy *et al.*, 2005). For example, Lu *et al.*, (2012) examined the carbothermal reductive upgrading of a bauxite ore using charcoal as a reductant and microwave radiation. They reported a successful separation of a magnetic fraction from a nonmagnetic fraction along with the formation of hercynite ($FeAl_2O_4$).

The reduction of iron oxide by postconsumer plastics has been investigated recently by some researchers, among which are Matsuda *et al*., (2006), Matsuda *et al*., (2008), Ueki *et al*., (2008), Dankwah *et al*., (2011), Nishioka *et al*., (2007), Dankwah *et al*., (2012), Dankwah *et al*., (2013), and Dankwah, 2014. However, the reduction of iron oxides from low-grade bauxite using postconsumer plastics as reductants has not been investigated before. Accordingly, in this investigation the aim is to generate carbonaceous materials from waste pure water sachets (PWS) for their subsequent utilisation as reductant for the upgrading of bauxite. Further, the effect of PWS on hercynite formation is examined.

2 Materials and Methods Used

2.1 Materials

The bauxite sample used in the study was provided by the Ghana Bauxite Company, Awaso, in Ghana (Fig. 1), while the source of carbonaceous materials was waste pure water sachets that were collected from various households in Tarkwa.

Fig. 1 Bauxite-Rich Areas in Ghana (Adapted from Dodoo-Arhin *et al.*, 2013)

The raw bauxite sample was crushed to particle size of 100% passing 2000 µm and. a representative sample was pulverised using a RETSCH pulveriser model 5657. The pulverised sample was then characterised by XRD using an EMPYREAN Diffractometer with cobalt as the source of x-rays and by XRF using X-ray Fluorescence SPECTROX-LAB-2000. The morphology of the bauxite sample was observed by SEM. Samples of waste pure water sachets were first heat-treated and then quenched to render them brittle. This was followed by pulverisation in RETSCH pulveriser model 5657. Size analysis of the pulverised sachets was conducted using a nest of sieves with 250 µm as the topmost sieve. The chemical compositions (elemental and proximate analyses) of PWS are shown in Table 1 and Table 2. The pulverised PWS sample was also characterised by XRD using an EMPYREAN Diffractometer. The XRF analysis of bauxite is presented in Table 3, which shows that the bauxite is low grade and the major impurity is iron oxide.

Table 2 Chemical Composition of PWS as Revealed by XRF

Component	C	H	S	N	O	Moisture	Ash
wt. %	72.32	12.8	0.28	0.23	4.76	2.87	6.3

Table 3 Ash Analysis of PWS as Revealed by XRF

Component	SiO_2	Fe_2O_3	Al_2O_3	TiO_2	P_2O_5	CaO	MgO
wt.%	41.45	10.79	6.77	2.82	0.82	26.60	2.14
Component	**Na_2O**	**K_2O**	**ZnO**	**CuO**	**SO_3**	**Mn_3O_4**	**SrO**
wt.%	1.95	2.56	0.43	0.37	1.45	0.37	0.12

Table 4: Chemical Composition of Awaso Bauxite Ore Utilised for the Investigation

Component	Composition (wt.%)
SiO_2	1.45
TiO_2	2.3
Al_2O_3	45
Fe_2O_3	25.88
CaO	0.08
MgO	0.11
MnO	0.03
V_2O_5	0.02
P_2O_5	0.15
Na_2O	0.06
LOI	24.95
TOTAL	**100.03**

Fig 2 (a) Waste Pure Water Sachets (b) Pulverised Carbonaceous Material obtained after Heat Treatment of Waste Pure Water Sachets

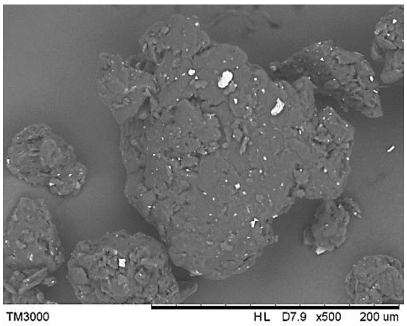

Fig. 3 SEM Photomicrograph of Pulverised Carbonaceous Material Generated from PWS

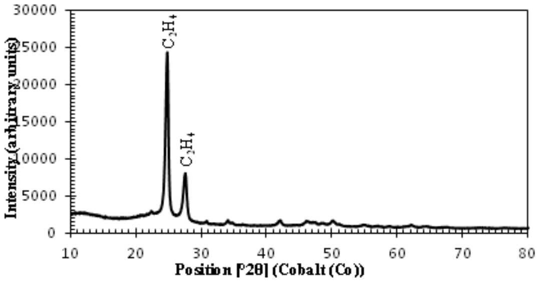

Fig. 4 XRD Diffraction Pattern of Pulverised Carbonaceous Material Generated from PWS Showing Crystalline Peaks identical to High Density Polyethylene (HDPE)

The reduction mixture was prepared by mixing raw materials (bauxite + pulverised PWS) without addition of any binder. Water was then added to the mixture and the entire mass was hand-rolled into pseudo-spherical pellets (micro-reactor).

Fig. 5 Bauxite-PWS Composite Pellet

The pellets were left in the open and allowed to cure and dry for 72 hours. The mass of the composite pellet was fixed (~51 g) and it was comprised of ~50 g of bauxite ore and ~1.0 g of pulverised PWS.

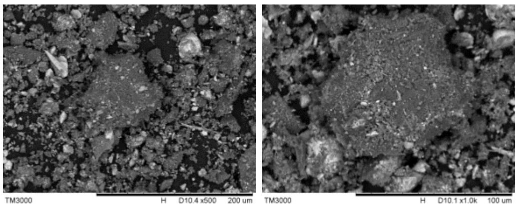

Fig. 6 SEM Photomicrograph of As-Received Awaso Bauxite Ore

2.2 Experimental Procedure

One composite pellet at a time was loaded into a fire clay crucible and placed at the central position of the ignited gas-fired furnace (Fig.7). The lid of the furnace was closed and firing commenced for 5, 10, 15, 20 and 30 minutes.

The sample was then removed, quenched, ground and separated into a nonmagnetic and magnetic fraction using hand-held low intensity magnet. The magnetic and non- magnetic portions were weighed separately using an electronic balance.

Fig. 7 Firing of Pellet in Progress

3 Results and Discussion

The following reactions are likely when a mixture of bauxite and pulverised PWS is heated:

(i) Thermal decomposition of PWS to generate CH_4, C and H_2

(ii) Conversion of goethite to hematite:

$$2\alpha\text{-FeOOH} = \alpha\text{-Fe}_2\text{O}_3 + \text{H}_2\text{O} \qquad (1)$$

(iii) Calcination of gibbsite, $Al_2O_3.3H_2O$ into alumina, Al_2O_3:

$$\text{Al}_2\text{O}_3.3\text{H}_2\text{O} = \text{Al}_2\text{O}_3 + 3\text{H}_2\text{O} \qquad (2)$$

(iv) Reduction of Fe_2O_3 to Fe_3O_4 by CH_4, C and H_2:

$$3\text{Fe}_2\text{O}_3 + \text{CH}_4 = 2\text{Fe}_3\text{O}_4 + \text{CO} + 2\text{H}_2 \qquad (3)$$

$$3\text{Fe}_2\text{O}_3 + \text{C} = 2\text{Fe}_3\text{O}_4 + \text{CO} \qquad (4)$$

$$3\text{Fe}_2\text{O}_3 + \text{H}_2 = 2\text{Fe}_3\text{O}_4 + \text{H}_2\text{O} \qquad (5)$$

(v) Formation of hercynite, $FeAl_2O_4$:

$$\text{Fe} + \text{Al}_2\text{O}_3 + ½\,\text{O}_2 = \text{FeAl}_2\text{O}_4 \qquad (6)$$

Hercynite formation during the carbothermal upgrading of bauxite has been reported by Lu *et al*, 2012. The free energy change for the formation of hercynite according to equation 6 varies with temperature (T≥1536 °C, i.e. above the melting point of metallic iron) as follows (Barin, 1995):

$$\Delta G^{o} = -328\,348 + 82.044\,T \ \text{J.mol}^{-1} \qquad (7)$$

The ternary system $FeO\text{-}Al_2O_3\text{-}SiO_2$ is shown in Fig. 8 displaying the stability regions at different compositions (Kapilashrami *et al.*, 2004). The mineral assemblages likely to form at temperatures below 900 °C are displayed in Fig. 9, (Levin *et al.*, 1964).

The free energy change in equation 7 and the ternary systems in Figs (8 and 9) indicate that hercynite formation is spontaneous under the experimental temperatures chosen for the current investigation. However, the extent of its formation will depend on the type and amount of reductant utilised for the process. The formation of hercynite during the carbothermal upgrading of bauxite is undesirable because it represents a loss in the amounts of both bauxite and alumina that could be separated, since it is nonmagnetic.

The chosen experimental temperature range (500-900°C) was such that SiO_2, TiO_2 and Al_2O_3 will remain immune to reduction by C, CO, H or CH_4, as higher equilibrium temperatures are required for their reduction by any of the reductants.

Transformation of goethite and hematite into magnetite commences as early as 5 minutes of firing, evidenced by the appearance of some peaks of Fe_3O_4 in Fig. 11 and the disappearance of some of the peaks of Fe_2O_3, which were originally present in Fig. 10. Several peaks of Fe_2O_3 and some C are also seen, an indication that the transformation of Fe_2O_3 to Fe_3O_4 is incomplete after 5 minutes. Calcination of part of the Gibbsite, $Al(OH)_3$, into alumina, Al_2O_3, is also observed, evidenced by the appearance of peaks of Al_2O_3 and the disappearance of some of the peaks of $Al(OH)_3$.

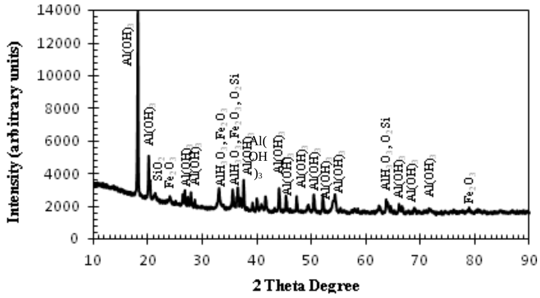

Fig. 10 XRD Diffraction Patterns of As-Received Awaso Bauxite

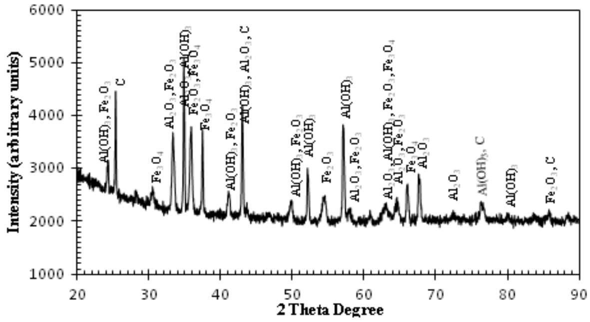

Fig. 11 XRD Diffraction Patterns of Crushed Pellet after Five Minutes of Firing

The SEM of the reduced pellet after five minutes is shown in Fig. 12. The morphology gives an indication of a dense structure, with no specific shape. In this period, melting of the polymer would have commenced along with partial reduction of Fe_2O_3 produced from the transformation of goethite. The reduction of Fe_2O_3 by the polymer and transformation of goethite and gibbsite are accompanied by the evolution of H_2O , which can contribute to initial densification of the fine particles Sintering of fine particles is highly favoured within this period, depending on the temperature, the type and amount of carbonaceous materials available for reduction.

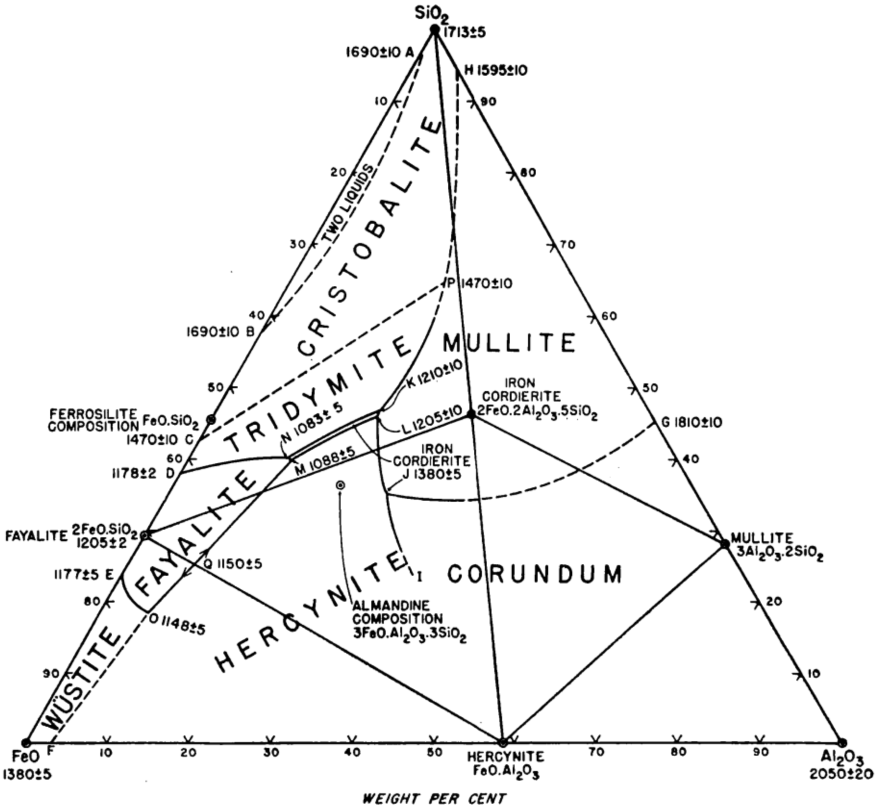

Fig. 8 Equilibrium Diagram of the System FeO-Al_2O_3-SiO_2, showing Fields of Primary Crystalline Phases, Tie Lines and Invariant Points (Kapilashrami *et al.,* 2004)

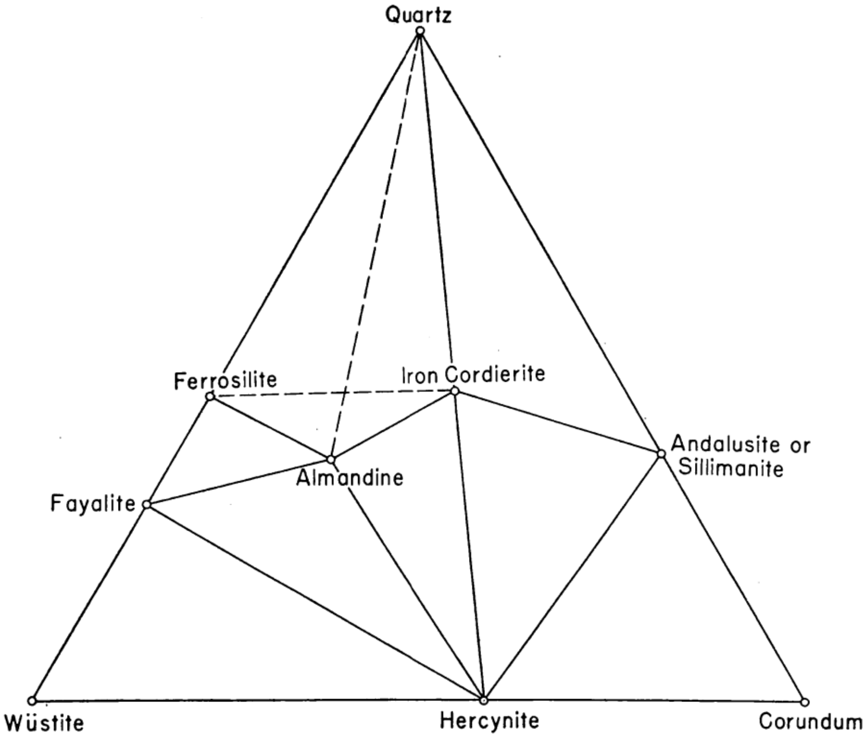

Fig. 9 Mineral Assemblages of the System FeO-Al_2O_3-SiO_2 below 900 °C (Levin *et al.,* 1964)

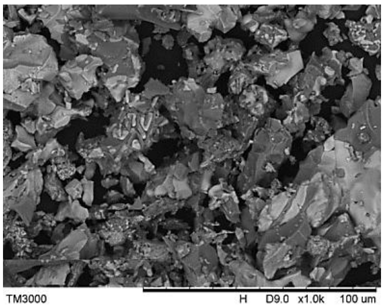

Fig. 12 SEM Photomicrograph of Awaso Bauxite Ore after Five Minutes of Heating with PWS

A photo and SEM of the magnetic fraction obtained after 30 minutes of firing are shown in Fig. 13, while the XRD is shown in Fig. 14. As shown in Fig. 14, the magnetic fraction shows distinct peaks of magnetite, indicating that Fe_2O_3 and FeOOH are transformed effectively into Fe_3O_4 by the carbonaceous material generated from PWS.

(a) (b)

Fig. 13 (a) Photograph and (b) SEM Photo-micrograph of Magnetic Fraction obtained after Heating Awaso Bauxite Ore with PWS

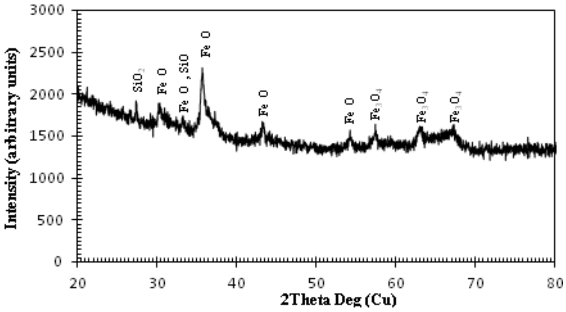

Fig. 14 XRD Diffraction Patterns of Magnetic Fraction Separated after Heating Awaso Bauxite Ore with PWS

A photo and SEM of the nonmagnetic fraction obtained after 30 minutes of firing are shown in Fig. 15, while the XRD is shown in Fig. 16. As would be expected, the nonmagnetic fraction consists of peaks of Al_2O_3 and SiO_2.

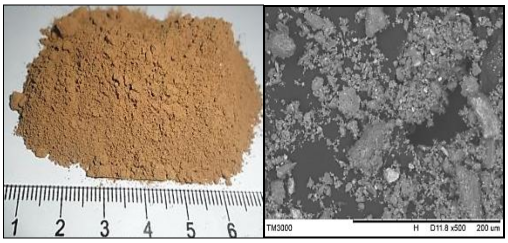

(a) (b)

Fig. 15 (a) Photograph and (b) SEM Photo-micrograph of Nonmagnetic Fraction obtained after Heating Awaso Bauxite Ore with PWS

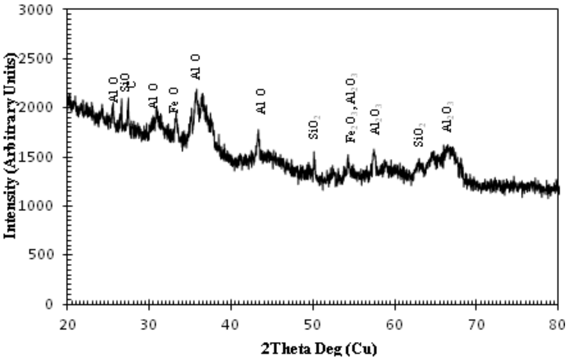

Fig. 16 XRD Diffraction Patterns of Non-magnetic Fraction Separated after Heating Awaso Bauxite Ore with PWS

Peaks in Fig. 14 and, especially, Fig. 16 are not as distinct as would be expected of crystalline materials, similar to the observation by Samouhos *et al., 2013*. The reduced mass was quenched rapidly after the heating process to prevent or minimise re-oxidation of Fe_3O_4 to Fe_2O_3. This rapid quenching could have contributed to the apparent non-crystallinity observed in several regions of especially, Fig. 16. From Figs 11, 14 and 16, it is apparent that hercynite ($FeAl_2O_4$) formation is absent in this investigation, contrary to the observation by Lu *et al* (2012).

The SEM/EDS of two regions of the non-magnetic fraction are shown in Figs 17 and 18. Both reveal high peaks of Al and O, suggesting that the non-magnetic fraction consists predominantly of Al_2O_3.

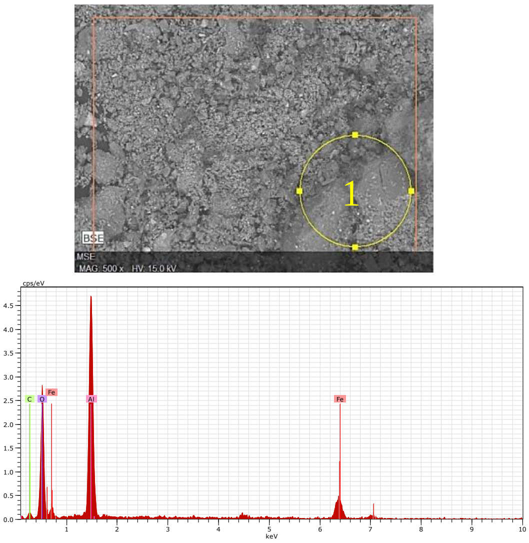

Fig. 17 SEM/EDS of Region 1 of Nonmagnetic Fraction obtained after Heating Awaso Bauxite Ore with PWS

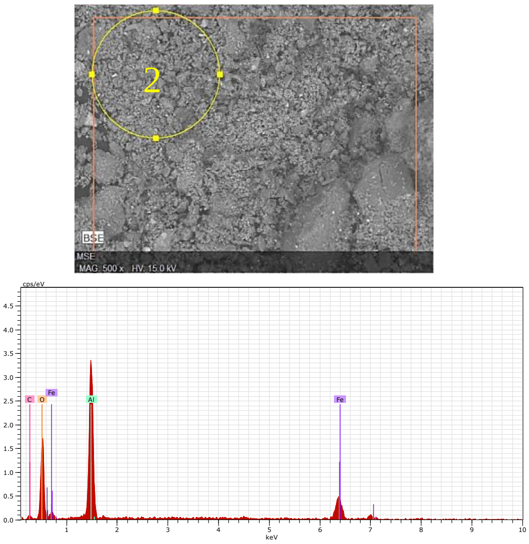

Fig. 18 SEM/EDS of Region 2 of Nonmagnetic Fraction obtained after Heating Awaso Bauxite Ore with PWS

The maximum amount of magnetite that can be separated into the magnetic fraction is about 12.5g, assuming that all the goethite and hematite are converted, based on the XRF data in Table 2. Of course, this excludes any contributions of oxides of iron from the ash of PWS. In the same vein, since alumina is not expected to undergo any reduction reaction, the content of alumina in the nonmagnetic fraction is about 22.5 g, in the absence of hercynite formation. The amount of magnetic material separated is shown as a function of time for various size ranges in Fig. 19. The mass of magnetic material recovered increased with time for all particle size ranges. The maximum amount of magnetic material separated was about 12.31 g and it was observed at a particle size of 180 µm.

For particle size finer than 180 µm, the amount of magnetic material separated decreased with a decrease in particle size, probably due to sintering effects, as shown in Fig. 20. Occlusion of magnetic material by a thick layer of nonmagnetic material can occur during sintering. Such occluded materials could be missed by a low intensity magnet similar to what was used in this investigation. The percent Al_2O_3 in the nonmagnetic fraction as a function of time is shown in Fig. 21 for various size ranges. The percent Al_2O_3 in the nonmagnetic fraction increased with time for all particle size ranges. It also increased with increasing fineness of the bauxite down to a particle size of 180 µm, beyond which it decreased with decreasing particle size.

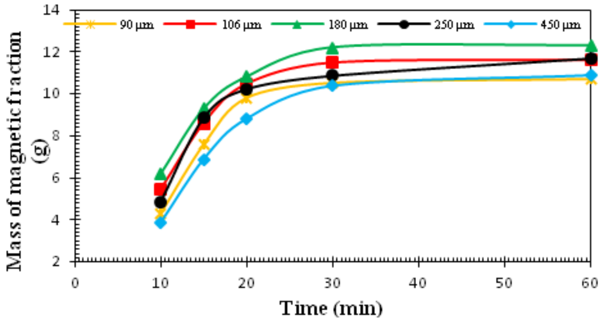

Fig. 19 Mass of Magnetic Fraction Removed as a Function of Firing Time

Fig. 20 Extremely Sintered Bauxite-Polymer Composite

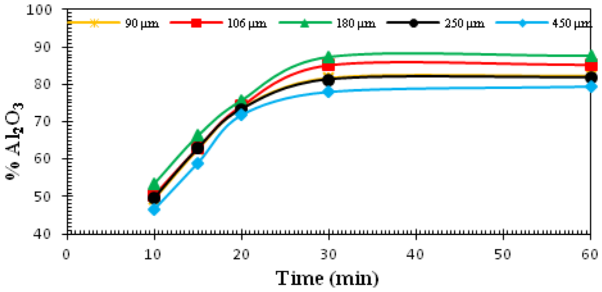

Fig. 21 Grade of Alumina in the Nonmagnetic Fraction as a Function of Firing Time

It is clear from the forgoing discussions that waste pure water sachets can be easily converted into an effective reductant for the subsequent upgrading of low-grade bauxite ore.

4 Conclusions

The upgrading of the Awaso bauxite has been investigated using carbonaceous material prepared from PWS. Major findings of the investigation are:

(i) Low grade Awaso bauxite ore can be upgraded successfully using carbonaceous materials generated from waste PWS.

(ii) XRD analysis revealed that PWS are semi-crystalline and are characterised by peaks identical to HDPE.

(iii) The maximum amount of magnetic fraction recovered was about 12.31g; this corresponds to over 90 % removal of the iron oxide content of the bauxite.

(iv) A mass balance analysis of the non-magnetic fraction reveals that the Awaso bauxite ore could be upgraded from a low grade of about 45 wt.% into a non-magnetic fraction of up to about 88 wt.% Al_2O_3.

(v) The use of PWS as a reductant precludes the possibility of hercynite formation that was reported by other investigators.

Acknowledgements

Part of the analyses for the investigation was conducted at the School of Materials Science and Engineering and the Analytical Centre, School of Chemical Science and Engineering, UNSW, Sydney, Australia. The authors are grateful to the various authorising bodies for the assistance received.

References

Barin, I. (1995), *Thermochemical Data of Pure Substances*, 3rd ed., VCH Pub. Inc., 1870 pp.

Dankwah, J.R., Koshy, P., Saha-Chaudhury, N.M., O'Kane, P., Skidmore, C., Knights, D. and Sahajwalla, V. (2011), “Reduction of FeO in EAF Steelmaking Slag by Blends of Metallurgical Coke and Waste Plastics”, *ISIJ Int*., Vol.51, No. 3, pp. 498-507.

Dankwah, J.R., Koshy, P., O’Kane, P. and Sahajwalla, V. (2012), “Reduction of FeO in EAF Steelmaking Slag by Blends of Metallurgical Coke and End-of-Life Tyres”, *Steel Research International*, Vol. 83, No.8, pp. 766-774.

Dankwah, J.R., Koshy P. and Sahajwalla, V.H. (2013), “Reduction of FeO in EAF Steelmaking Slag by Blends of Metallurgical Coke and End-of-Life Polyethylene Terephthalate”, *Ironmaking and Steelmaking*, Vol. 41, No. 6, pp. 401-409.

Dankwah, J. R., and Koshy, P. (2014), “Reduction of FeO in EAF Steelmaking Slag by Blends of Metallurgical Coke and Waste Polypropylene”. *High Temperature Materials and Processes*, Vol. 33, No. 2, pp. 107-114.

Dodoo-Arhin, D., Konadu, D. S., Annan, E., Buabeng, F. P., Yaya, A. and Agyei-Tuffour, B. (2013), “Fabrication and Characterisation of Ghanaian Bauxite Red Mud-Clay Composite Bricks for Construction Applications”, *American Journal of Materials Science*, Vol 3, No. 5, pp. 110-119.

Kapilashrami, E., Sahajwalla, V., and Seetharaman, S. (2004), “Slag Formation during High-Temperature Interactions between SiO_2-Containing Refractories and Iron Melts with Oxygen”. *VII International Conference on Molten Slags Fluxes and Salts*, The South African Institute of Mining and Metallurgy, CD-1.

Kesse, G. O. (1985), *The Mineral and Rock Resources of Ghana*, A. A. Balkema, Publishers, Rotterdam, 610 pp.

Levin, E. M., Robbins, C. R., and Mcmurdie, H. F. (1964), *Phase Diagrams for Ceramists*, Reser, M. K (ed.), Ohio, The American Ceramic Society, pp. 696.

Lu, T., Pickles, C. A. and Kelebek, S. (2012), “Carbothermal Reductive Upgrading of a Bauxite Ore using Microwave Radiation”, *High Temp. Mater. Proc.*, Vol. 31, No. 2, pp. 139-148.

Lu, T., Pickles, C.A. and Kelebek, S. (2007), Symposium on Light Metals in Transport Applications, Edited by Bekguleryuz, M.O., Paray, F. and Wells, M. Conference of Metallurgists (CIM), Toronto, Canada, pp. 421-448.

Matsuda, T., Takekawa, M., Hasegawa, M., Ikemura, Y., Wakimoto, K., Ariyama, T., and Iwase, M. (2006), “Utilization of Waste Wood for Production of Iron, Carbon Monoxide and Hydrogen without Generating Carbon Dioxide”, *Steel Res. Int.*, Vol. 77, pp. 774-784.

Matsuda, T., Hasegawa, M., Ikemura, A., Wakimoto, K., and Iwase, M. (2008), “Utilization of Waste Plastic for Production of Metallic Iron, Hydrogen and Carbon Monoxide without Generating Carbon Dioxide”, *ISIJ Int.*, Vol. 48, No. 9, pp. 1186-1196.

Nishioka, K., Taniguchi, T., Ueki, Y., Ohno, K., Maeda, T., and Shimizu, M. (2007), "Gasification and Reduction Behaviour of Plastic and Iron Ore Mixtures by Microwave Heating", *ISIJ Int.*, Vol. 47, No. 4, pp. 602-607.

Reddy, B. R., Banarjee, G., Rao, R. T., Mishra, S. K., Dey, D. K., Beshra, L. and Ray, H. S. (2005), Indian Pat. Appl., 9 pp.

Samouhos, M., Taxiarchou, M., Tsakiridis, P. E. and Potiriadis, K. (2013), "Greek Red Mud Residue: A Study of Microwave Reductive Roasting followed by Magnetic Separation for a Metallic Iron Recovery Process", *Journal of Hazardous Material*, pp. 194-205.

Ueki, Y., Ohno, K., Maeda, T., Nishioka, K., and Shimizu, M. (2008), "Reaction Behaviour during Heating Waste Plastic Materials and Iron Oxide Composites", *ISIJ Int.*, Vol. 48, pp. 1670-1675.

Yeh, C. H. and Zhang, G. (2013), "Stepwise Carbothermal Reduction of Bauxite Ores", *International Journal of Mineral Processing*, Vol. 124, pp. 1-7.

Authors

Dr James R. Dankwah had his Ph.D. from the School of Materials Science and Engineering, UNSW-Australia in 2012. He is currently a Senior Lecturer and Head of Minerals Engineering Department, University of Mines and Technology (UMaT), Tarkwa. His current research areas include iron and steelmaking, high-temperature metallurgical processes, and utilisation of waste polymers in metal extraction processes. He has over 30 refereed journal and conference papers.

Allen Y. Fosu had his BSc degree in Chemistry from the Kwame Nkrumah University of Science and Technology, Kumasi. He is currently a postgraduate student at the Minerals Engineering Department, University of Mines and Technology, Tarkwa. He is currently working on carbothermal upgrading of the Awaso Bauxite ore using waste polymers and biomass as reductants.

Nelson Fosu is a final year undergraduate student at the Minerals Engineering Department, University of Mines and Technology, Tarkwa, Ghana. He is currently working on the carbothermal upgrading of Awaso Bauxite using pure water sachets as reductant.

Dr. Pramod Koshy completed his Ph.D. from the School of Materials Science and Engineering, UNSW- Australia in 2009. He is currently a Senior Research Associate at the School. His main areas of research include photocatalytic materials, high-temperature metal/ceramic interfaces, and utilization of waste materials. He has over 40 refereed journal papers, one international patent, and over10 conference proceeding papers.